Journal of
Water, Sanitation & Hygiene for Development

IWA PUBLISHING

 Journal of Water, Sanitation and Hygiene for Development Vol 11 No 6, 1083 doi: 10.2166/washdev.2021.117

Research Paper

Removal of metronidazole antibiotic from aqueous solution by ammonia-modified activated carbon: adsorption isotherm and kinetic study

Ali Ahmadfazeli[a], Yousef Poureshgh[b], Yousef Rashtbari[b], Hamed Akbari[a], Peyman Pourali[b] and Amir Adibzadeh [a,c,*]

[a] Health Research Center, Lifestyle Institute, Baqiyatallah University of Medical Sciences, Tehran, Iran
[b] Department of Environmental Health Engineering, School of Health, Ardabil University of Medical Sciences, Ardabil, Iran
[c] Department of Environmental Health Engineering, School of Public Health, Baqiyatallah University of Medical Sciences, Tehran, Iran
*Corresponding author. E-mail: rsr.adibzadeh@bmsu.ac.ir

AA, 0000-0002-5703-0759

ABSTRACT

This article was aimed at investigating the removal of metronidazole (MNZ) from aquatic solutions by modified activated carbon (MAC) with amine groups. The effect of various parameters on the adsorption rate such as the initial pH, adsorbent dose and initial concentration of MNZ and contact time were scrutinized. MAC was characterized by Fourier transform infrared spectroscopy and Brunauer–Emmett–Teller techniques. The obtained results illustrated that under the optimum conditions (pH = 3, contact time = 50 min, initial MNZ concentration = 5 mg/L and MAC dose = 0.5 g/L), the maximum adsorption efficiency was 95%. Furthermore, the kinetic studies indicated the applicability of the pseudo-second-order kinetic model, whereas the adsorption isotherm fitted well with the Freundlich model (0.996), and the maximum adsorption capacity was 66.22 mg/g. The S_{BET} and the total pure volume of MAC were 706.92 m^2/g and 0.532 cm^3/g, respectively. Also, the regeneration tests demonstrated that MAC had good stability after five cycles (73%). It can be concluded that MAC, as an effective adsorbent, has a high ability to remove MNZ from aqueous solutions.

Key words: adsorption isotherm, kinetic, metronidazole antibiotic, modified activated carbon

HIGHLIGHTS

- MNZ Adsorption was high in acidic conditions.
- MNZ removal performance decreased with increasing initial MNZ concentration.
- MNZ adsorption was well proportionated with the pseudo-second-order and Freundlich models.
- MAC regeneration showed that this adsorbent has promising capacity in five regeneration cycles for MNZ removal.

GRAPHICAL ABSTRACT

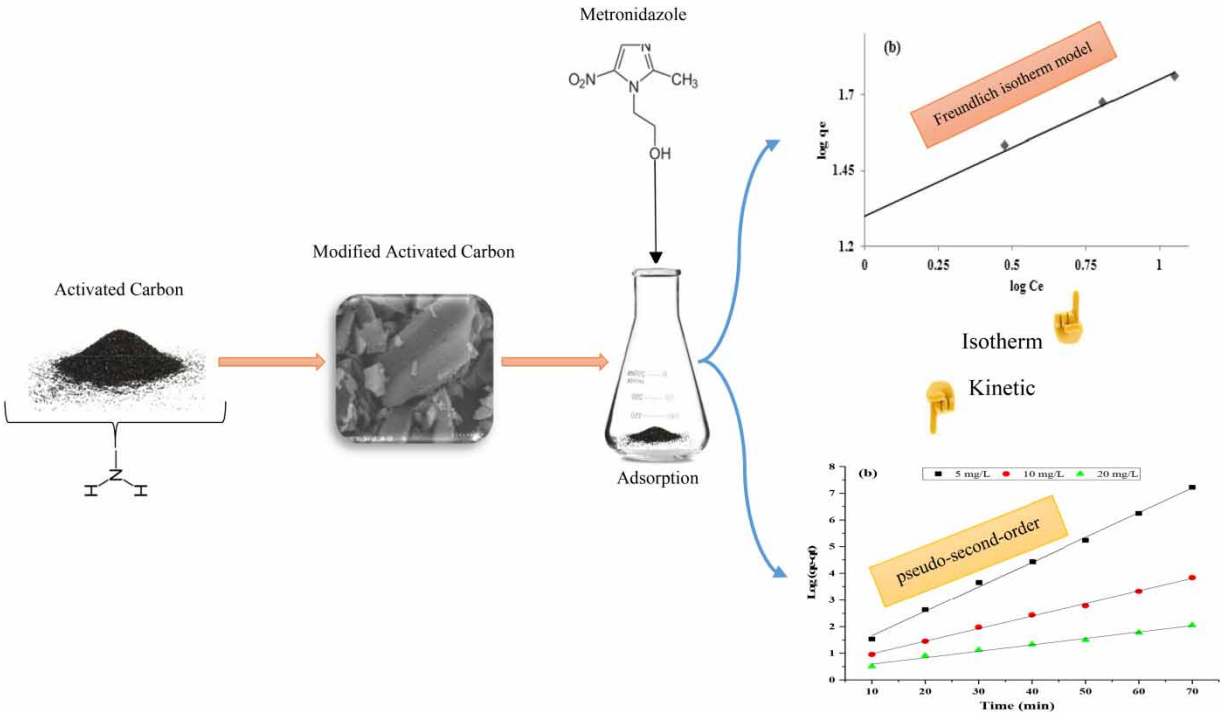

1. INTRODUCTION

Industrial wastewaters contain toxic, carcinogenic and mutagenic compounds, and the removal of these pollutants from the produced effluents is of particular importance (Albadarin *et al.* 2012; Akbari & Adibzadeh 2020). One of the priority pollutants is pharmaceutical compounds that get into the surface and groundwater mainly through discharging industrial and municipal wastewaters (Bahrami Asl *et al.* 2015; Dong *et al.* 2016). The presence of medicinal substances in the environment due to their high stability disrupts the conventional wastewater treatment processes (Rivera-Utrilla *et al.* 2009; Alinejad *et al.* 2019).

Approximately 30–90% of antibiotics consumed by human beings and animals are not metabolized in the body and excreted out without any change into sewerage. Furthermore, conventional wastewater treatment processes can only remove a range of 60–90% of some antibiotics; this results in increased bacterial resistance in the environment and, in turn, different diseases if antibiotics are transmitted to human body (Rashtbari 2020a).

The entrance of pharmaceutical substances, antibiotics and their metabolites into aqueous media has been the source of concerns in recent years (Joss *et al.* 2006). Antibiotics are stable and lipophilic and preserve their chemical structure for a long time in the body for therapeutic purposes. Then, the application of wastewater and its fertilizer in the soil can cause environmental pollution (Shokoohi *et al.* 2018b; Rahmani *et al.* 2019). The constant presence of antibiotics in the environment, the food chain, the aquatic environment and their bioaccumulation leads to microbial and bacterial resistance (Watkinson *et al.* 2007). Although the environmental concentration of antibiotics is very low, they can threaten human health due to bacterial resistance. Studies have shown that antibiotics are absorbed in small amounts in the body, and most of which are excreted from the body (Shemer *et al.* 2006; Shokoohi *et al.* 2018a).

One of the most widely used antibiotics is anti-bacterial and anti-inflammatory metronidazole (MNZ), which is utilized for the treatment of diseases in addition to being used as an additive and anti-parasite in poultry and fish food. This antibiotic has a circular structure due to the destruction of DNA in lymphocytes, which has the potential for mutagenicity and carcinogenicity. According to the International Agency for Research on Cancer (IARC), the mutagenicity of MNZ has been confirmed in the bacterial system and its carcinogenicity in animals and its toxicity on the human genome (Kümmerer *et al.* 2000; Fang *et al.* 2011).

Several methods such as the direct UV photolysis (Dantas *et al.* 2010), ozonation process (Kermani *et al.* 2013), solar photoelectro-Fenton (Pérez *et al.* 2015), bio sorbent (Azarpira & Balarak 2016), photocatalytic process (Wang *et al.* 2010) and adsorption- process (Carrales-Alvarado *et al.* 2014) have been employed for the removal of MNZ from aqueous solutions. However, most of the mentioned methods are not suitable due to low efficiency, high operational cost and high energy requirement, and some of them are not eco-friendly (Jung *et al.* 2013). Among these methods, the adsorption process benefits from some unique advantages such as low costs, high flexibility, simple navigation, insensibility, high capability, reusability and eventually recycling of valuable pollutants (Su *et al.* 2011). Activated carbon as a sorbent is a suitable alternative for the effective removal of organic pollutants from aqueous media along with the porosity structure and high surface area. But the problems such as filtration, dispersion and turbidity, and the high cost of recovery lead to its application restriction on large scales (Ai & Jiang 2010). Recently, the modification of activated carbons with different methods has been applied to overcome its circumscription. The main reason for surface oxidation and the development of oxygen surface groups is the role of these functionalities as an intermediate stage to develop some oxygenated anchoring sites before introducing nitrogen functionalities to carbon surface (Pittman *et al.* 1997). When oxidized carbons are treated via ammonia at high temperatures, free radicals (such as NH_2, NH and atomic hydrogen), which are created during ammonia decomposition, may attack the surface oxides and active sites present on the carbon surface to form nitrogen-containing functional groups (Stöhr *et al.* 1991; Shafeeyan *et al.* 2011). Numbers of studies have reported on the use of different adsorbents for the removal of MNZ from aqueous solutions. Flores-Cano *et al.* investigated the removal of MNZ on activated carbons derived from coffee residues and almond shells (Flores-Cano *et al.* 2016). In another research, Sun *et al.* studied the adsorption of MNZ onto biochar derived from Sugarcane Bagasse (Sun *et al.* 2018). However, there is no report on the removal of MNZ by functionalization of commercial activated carbon using ammonia. Therefore, the aim of this study was to investigate the performance of functionalization of commercial activated carbon using ammonia for the removal of MNZ from aquatic solutions.

2. MATERIALS AND METHODS

2.1. Reagents, materials and solutions

In this study, all chemicals materials were purchased from Merck, and MNZ of purity 97% ($C_6H_9N_3O_3$; MW = 171.2 g/mol) was bought from Sigma Aldrich Co in Iran. Table 1 shows the characteristics and chemical structure of MNZ (Shemer *et al.* 2006; Zarei *et al.* 2018). Also, H_2SO_4 and NaOH were obtained from Merck Germany laboratory with a degree of purity to adjust the pH of the solution. The stock of synthetic MNZ (1,000 mg/L) was made by dissolving the required amount in deionized water and was kept in a glass container and kept in the dark at below 4 °C. It should be noted that in all stages of the experiments, double distilled water was used.

2.2. Preparation of modified activated carbon

All of the required activated carbons were prepared from Merk Company. First, for the production of soluble mediator's amine, 98 mL of chlorohydrin solution was contacted with 152 mL of diethylamine solution in 150 mL of dimethylformamide (DMF) into an evaporator at 85 °C for 120 min. In the second step, to make modified activated carbon (MAC), 20 g of

Table 1 | Characteristics and structure of MNZ

Molecular structure	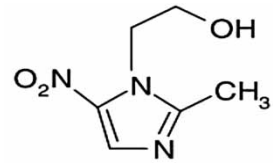
Molecular formula	$C_6H_9N_3O_3$
Molecular weight (g/mol)	171.2
Melting point (°C)	159–163
Water solubility (g/L)	9.5
pKa	2.55

powdered activated carbon (PAC) was mixed with 60 mL of the prepared amine solution, and 20 mL of pyridine was used as a catalyst. This stage was performed in an evaporator at 80 °C for 2 h. Next, for the elimination of residual chemicals, MAC was washed with 0.1 N HCl and NaOH, and after that, distilled water was used for further cleanup of the adsorbent; then, natural pH was achieved. Finally, the synthesized MAC was dried at 50 °C in 24 h and then stored for further use (Gholami *et al.* 2018).

2.3. Characterization of MAC

The Fourier transform infrared spectroscopy (FTIR, Perkin Elmer) was prepared by using potassium bromide (KBr) as the reference and analyzed with a 1 cm^{-1} resolution in a wide range of frequency of 450–4,000 cm^{-1}. The nitrogen adsorption/desorption isotherms were conducted by the Brunauer–Emmett–Teller (BET) analysis (II BELSORP mini) at 77 K to determine the pore volume and specific surface area of MAC. The point of zero charge (pH_{pzc}) was investigated for the determination of adsorbent surface charge. The scanning electron microscope (SEM) images of the samples were obtained on a MIRA3 TESCAN at an accelerating voltage of 30 kV. X-ray diffractometer (XRD) analysis was examined with US Intel diffractometer EQuniox 3000 in the 2θ range between 10 and 80° with a scanning speed of 0.01 to ensure the formation of the activated carbon.

2.4. Adsorption experiments

The effect of experimental parameters, namely, pH (3, 5, 7, 9 and 11), adsorbent dose (0.1, 0.25, 0.5, 0.75 and 1 g/L), contact time (10, 20, 30, 40, 50, 60 and 70 min), initial concentration (5, 10, 20, 30 and 40 mg/L) and regeneration, was studied. The pH of the solution for each experiment was adjusted by using 0.1 M NaOH or H_2SO_4. The solutions were agitated for achieving equilibrium time at room temperature at a constant speed (250 rpm). After the completion of the reaction time, centrifugation was done to isolate the solvent absorber with 5,000 rpm for 10 min and filter using a Whatman paper (0.2 μm), and then the filtered sample was analyzed by a UV–visible spectrophotometer (model DR 5000) at the maximum absorption wavelength to determine the residual MNZ concentration. After equilibrium, the removal efficiency and the adsorption capacity (q_e, mg/g) were calculated using the following equations, respectively (Afshin *et al.* 2019; Rashtbari *et al.* 2020a, 2020b):

$$\text{Removal efficiency } (\%) = \left(\frac{C_o - C_e}{C_e}\right) \times 100 \tag{1}$$

$$\text{Adsorption capacity, } q_e = \frac{(C_o - C_e) \times V}{M} \tag{2}$$

where C_o and C_e are the initial dye concentration and the MNZ concentration at the time of equilibrium (mg/L), V is the volume of the solution (L) and M is the mass of the adsorbent (g).

2.5. Determination of MNZ concentration

The measurement of MNZ concentration in this study was carried out using a UV–visible spectrophotometer (model DR 5000) at 320 nm wavelength according to the Standard Methods for the Examination of Water and Wastewater (Nasseh *et al.* 2019).

2.6. Determination of pH_{pzc}

One of the most important characteristics of the adsorbents is pH_{pzc}, showing the state of electrical charge dispersion on the adsorbent surface. To determine pH_{pzc}, 30 mL of a 0.1 M solution of sodium salt was poured into 11 100-mL Erlenmeyer flasks, and the pH values of the solutions were adjusted between 2 and 12. Then, 0.05 g of the MAC prepared in each of the flasks was added. Next, the solutions were placed on a shaker at a speed of 250 rpm for 48 h. Later, the final pH of the solutions was measured after the adsorption separation. Finally, pH_{pzc} was determined after plotting the final pH change curve against the initial pH (Rivera-Utrilla *et al.* 2010).

3. RESULTS AND DISCUSSION

3.1. Determination of the structural characteristics of the adsorbent

To study the nature of the functional groups, present on the surface of the samples, the FTIR analysis was carried out. Figure 1(a) shows the results of FTIR measurements taken for the untreated carbon and modified with amine groups samples.

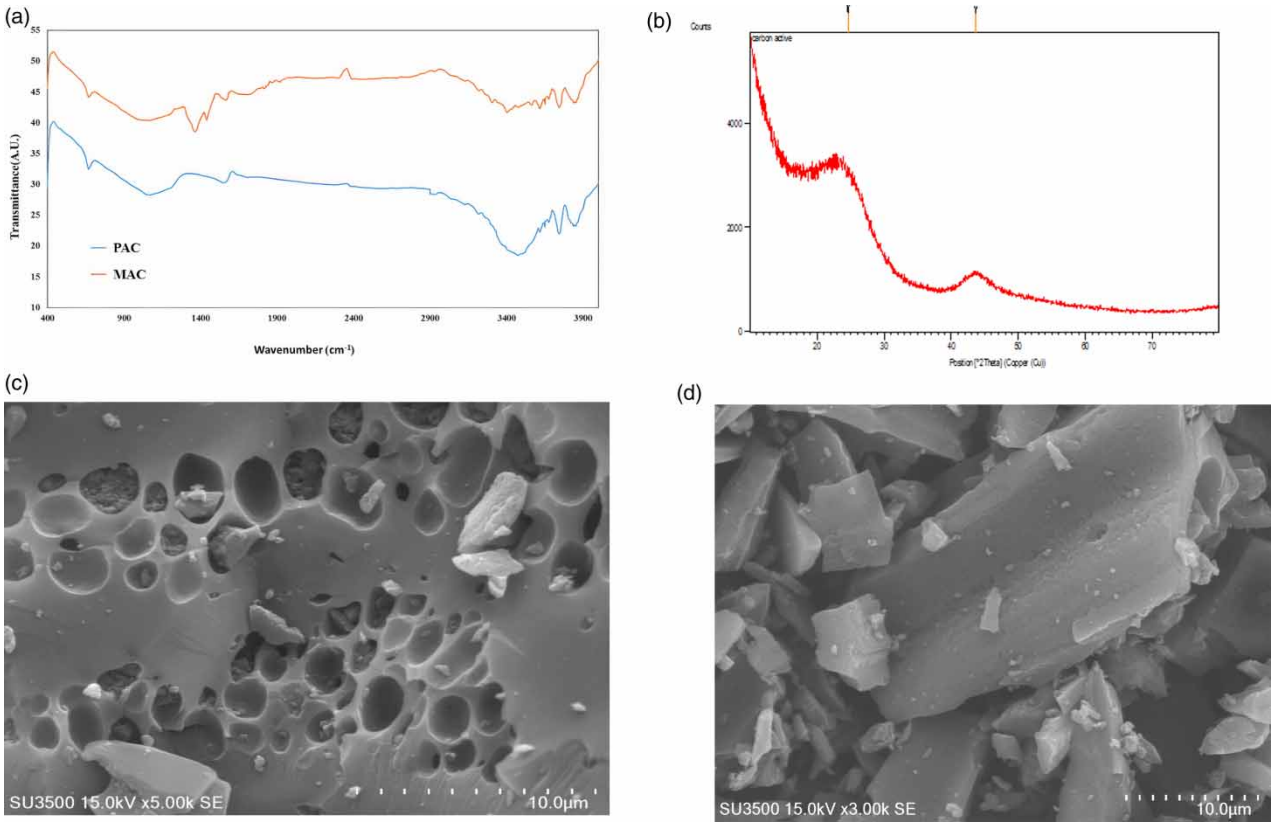

Figure 1 | FTIR spectra PAC and MAC (a), typical XRD patterns of MAC (b) and SEM micrographs of PAC and MAC (c) and (d).

The broad peaks detected at 1,570–1,700 cm^{-1} were weaker because of the reduction of the C–O bond. As can be seen, there were a few weak peaks, corresponding to the existence of a few functional groups. The broad bands that appeared at 3,426 cm^{-1} for PAC could be attributed to O–H vibration in the H_2O molecule (Huang *et al.* 2014). Ammonia treatment caused some changes in the spectra of modified samples. In the range of 3,376–3,294, overlapping bands of O–H and N–H stretching vibrations were observed for all the modified samples (Shafeeyan *et al.* 2011). Absorption at wavenumbers of 2,930 cm^{-1} for PAC and 2,941 cm^{-1} for MAC are attributed to the aliphatic C–H interaction with the surface of the adsorbent (Moussavi *et al.* 2013). MAC displays the presence of one strong peak at 2,360 cm^{-1} which corresponds to the C–C stretching vibrations in alkyne groups. In addition, the spectrum of MAC exhibits the appearance of new bands related to the N-containing species at 1,542 cm^{-1} (cyclic amides and 1,052 cm^{-1}); C–N of the amine group implies that the use of ammonia modification produced new nitrogen surface complexes. The peak created around the 577.18 cm^{-1} bands relates to the presence of amine groups (CN tensile vibrations), which are coated on the activated carbon. Thus, the results of FTIR showed that amine groups were well coated on active carbon (Wang *et al.* 2007; Moussavi *et al.* 2013). Figure 1(b) shows the XRD patterns of MAC in the 2θ range from 20 to 80°. It was found that there was a series of conventional broad peaks at 23.1, 24.2 and 26.5° which are a special characteristic of the activated carbon (Xu *et al.* 2017). Figure 1(c) and 1(d) indicates the images of MAC and PAC by the SEM (Shemer *et al.* 2006). The SEM is a primary tool used for the characterization of the surface morphology and fundamental physical properties of adsorbent surfaces. It is useful for the determination of particle size, shape and porosity. The surface morphology of both adsorbents was investigated using SEM micrographs. The SEM micrograph of both carbon types (Figure 1(c)) indicated that PAC has a form like compressed and porous fibers with a series of parallel and long channels, but MAC (Figure 1(d)) had a smooth surface with scattered holes. In this study, the specific surface areas (S_{BET}) and pore size distribution of the adsorbents were calculated by the multipoint BET and Barrett–Joyner–Halenda methods. The specific surface area (S_{BET}) and pore volume of adsorbents have been compiled in Table 2. The results obtained showed that the *S*BET and the total pure volume for the MAC and PAC were 706.92, 738.18 m2 g−1 and 0.532, 0.551 cm^3 g^{-1}, respectively. It was found that modification slightly decreased the apparent surface area, total pore and micropore volumes.

Table 2 | BET – specific surface area (S_{BET}), total pore volume (V_{Total}), micropore volume (V_{micro}) and mesopore volume (V_{meso}) of PAC and MAC

D_p (nm)	V_{meso} (cm^3/g)	V_{micro} (cm^3/g)	V_{Total} (cm^3/g)	S_{BET} (m^2/g)	Material
PAC	738.18	0.551	0.2421	0.3354	3.08
MAC	706.92	0.532	0.2316	0.3241	3.1

For instance, the surface area of the modified adsorbent was 706.92 $m^2\ g^{-1}$, which represented 95.7% of the surface area of the untreated adsorbent. The decrease in porous texture properties is probably due to the partial blockage of the micropore entrances by nitrogen functional groups that occur during modification (Pereira *et al.* 2003). The MAC and PAC showed an average pore diameter of 3 nm, which can allow ions to penetrate easier into their porous surface.

3.2. Effect of solution pH

The initial pH is one of the main parameters that affect the adsorption process with the effect on solution chemistry and the activity of functional groups on absorbent surfaces. Figure 2 shows the effect of the pH of the solution on the removal of MNZ by MAC. Note that for the removal, the initial pH of the solutions was adjusted from 3 to 11 to determine the optimum pH. The efficiency declined with increasing the pH value. For example, at pH = 3 and 11, the percentages of MNZ removal were 97 and 65%, respectively. Therefore, pH = 3 was selected for the next experiments. This can be attributed to pH_{pzc} (pH value of zero charges, pH at which the flux transfer occurs from the surface). Normally, adsorption is fully dependent on the pH_{pzc} value of adsorbent, which in this study, was found to be 6.83 for MAC (Figure 2(b)); a positive charge developed on the surfaces at pH below pH_{pzc}. The high removal efficiency of antibiotics in acidic conditions indicates the adsorption of the contaminant on adsorbents through its carboxyl groups (Legnoverde *et al.* 2014). In basic conditions, the levels of electrostatic discharging strength between antibiotics and negative sites are reduced on the adsorbent surfaces, leading to a decrease in the removal efficiency of pollutants from the solution. The number of OH^- groups increased with increasing the pH of the solution, which generally resulted in a decrease in positive reception sites, and consequently, the effectiveness of MNZ elimination went down (Pouretedal & Sadegh 2014). The behavior of MNZ sorption with the changing pH in this study was similar to that reported by Wang who showed that the adsorption of MNZ, at pH values around 3.3–5, was higher than that of pH range from 3.33 to 9.30 (Wang *et al.* 2016).

3.3. Effect of adsorbent dosage

As shown in Figure 3, the amount of adsorbent dose is an important factor that affects the percentage of removal efficiency. In this study, the removal percentage of MNZ increased from 75 to 96% by raising the MAC dose from 0.1 to 0.5 g/L. The results of the present work indicated that the percentage of MNZ removal enhanced with increasing adsorbent dose. This can be

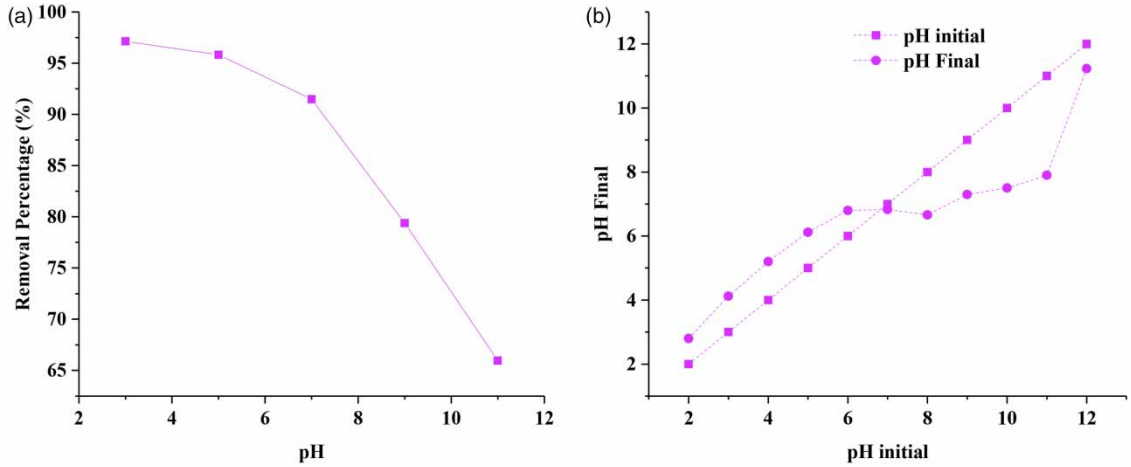

Figure 2 | Effect of pH on the adsorption of MNZ by MAC (contact time: 50 min, initial MNZ concentration: 5 mg/L, solution temperature: 25 °C, MAC dose: 0.5 g/L) (a) and pH_{pzc} (b).

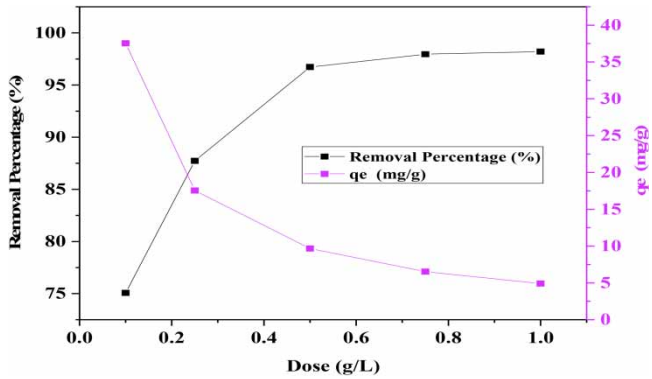

Figure 3 | Effect of adsorbent dosage on the adsorption of MNZ by MAC (contact time: 50 min, pH: 3, initial MNZ concentration: 5 mg/L).

attributed to the higher adsorbent surface area, as well as the availability of more binding sites due to an increase in the amount of absorbent dosage (Ghaedi *et al.* 2013). Furthermore, the absorption capacity reduced with an increase in dose, so that the absorption capacity of MNZ reduced from 37.54 to 4.91 mg/g in doses from 0.1 to 1 g/L. Therefore, 0.5 g/L of the adsorbent was selected as the optimal dose. Although with an increase in absorbent dose the removal efficiency increased due to the saturation of some sites on the adsorbent surface, the adsorption capacity decreased (Hoseinzadeh *et al.* 2013; Khosravi *et al.* 2018). The results of this study were consistent with the results obtained by Khosravi *et al.*, who used modified montmorillonite with ZnO and TiO_2 nanoparticles in the presence of H_2O_2 to absorb cephalexin from aqueous solutions; they reported that the percentage of cefalexin, which was %33, increased with increasing the amount of green local montmorillonite (GLM) from 0.4 to 4 g/L (Khosravi *et al.* 2018).

3.4. Effect of contact time and initial MNZ concentration

The contact time between absorbent and adsorbate as well as the initial concentration of MNZ are important parameters in the adsorption process. The effect of contact time on MNZ adsorption on MAC was examined at various concentrations of MNZ (Figure 4). The adsorption rate of MNZ at various initial concentrations was high during the first 10 min of the process and that is due to the high free space in the early stages of the process. After 10 min, the removal percentage reduced gradually. Generally, the ideal adsorbent adsorbs contamination at low contact times with high removal performance. The initial concentration is another important factor which affects the amount of adsorption of the MNZ from the solution. The MNZ elimination efficacy decreased by increasing initial concentrations. Accordingly, with an increase in the initial concentration of MNZ from 5 to 40 mg/L, the adsorption percentage decreased from 95 to 69.23% in 50 min; this indicates that the initial concentration strongly affects the removal efficiency. However, the equilibrium absorption capacity increased with an increase in the initial concentration of MNZ. It can also be explained by the fact that more binding sites are available

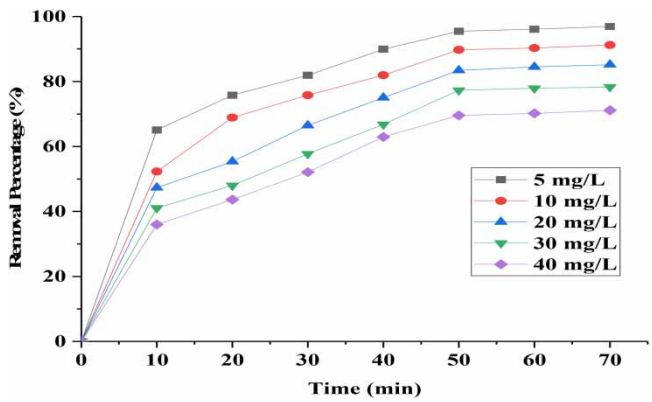

Figure 4 | Effect of the initial MNZ concentration and contact time on the adsorption of MNZ by MAC (contact time: 70 min, pH: 3, adsorbent dosage: 0.5 g/L).

when MNZ concentration is raised. This can lead to an increase in the concentrations of pollutants, which acts as a propulsion to overcome the resistance between the aqueous phase and the adsorbent (Pouretedal & Sadegh 2014). The results were consistent with other studies (Ahmed & Theydan 2012; Samarghandi *et al.* 2015). Mousavi *et al.* studied the antibiotic removal of amoxicillin by the NH_4Cl-MAC. They found that, by increasing the concentration of amoxicillin from 100 to 500 mg/L, the percentage of antibiotic removal of SAC and NAC decreased from 100 to 41% due to the saturation of accessible sites (Moussavi *et al.* 2013).

3.5. Isotherm studies

Adsorption isotherm studies indicate the relationships between the adsorbate and the absorbent; besides, it allows the determination of the theoretical maximum adsorption capacity of an adsorbent to a given adsorbate. To explain the adsorption behavior of MNZ on the MAC, the data from the adsorption equilibrium test stage were tested on the most common models: Langmuir and Freundlich. For the Langmuir isotherm, its linear relationship was used (Equation (3)) (Baocheng *et al.* 2008; Fazlzadeh *et al.* 2016; Afshin *et al.* 2018):

$$\text{Langmuir: } \frac{C_e}{q_e} = \frac{1}{K_L * q_{max}} + \frac{C}{q_{max}} \tag{3}$$

where C_e is the concentration of MNZ adsorption (mg/L), q_e is the amount of MNZ adsorbed per unit mass of MAC (mg/g) and K_L is the Langmuir constant (L/mg) and expresses the adsorption energy. The fundamental characteristics of the Langmuir isotherm can be expressed by the dimensionless reversible factor, R_L (Fazlzadeh *et al.* 2017):

$$R_L = \frac{1}{1 + (q_{max} * K_L) C_o} \tag{4}$$

here, if R_L is greater than 1, absorbance is unfavorable; if it is equal to 1, it is linear adsorption; if it is between 0 and 1, adsorption is favorable and if it is equal to 0, adsorption is irreversible.

The Freundlich isotherm shows heterogeneous and multi-layered adsorbent adsorption. For the Freundlich isotherm, its linear relationship was used (Equation (5)) (Abdollahzadeh *et al.* 2020):

$$\text{Freundlich: } \ln q_e = \ln K_F + \frac{1}{n} \ln C_e \tag{5}$$

where K_F expresses the maximum absorption capacity (mg/g), and $1/n$ expresses the adsorption intensity. If n is between 1 and 10, it indicates that the adsorption is favorable.

Figure 5 represents the Langmuir and Freundlich isotherms derived from the adsorption process data, and Table 3 shows the coefficients of adsorption isotherm models. As can be seen, the amount of R^2 for the MAC adsorbent in the Freundlich isotherm was higher than that in the Langmuir isotherm, indicating that the adsorption process followed the Freundlich model. Also, the value of R_L was between 0 and 1, which confirms that MNZ adsorption by the MAC was favorable. On

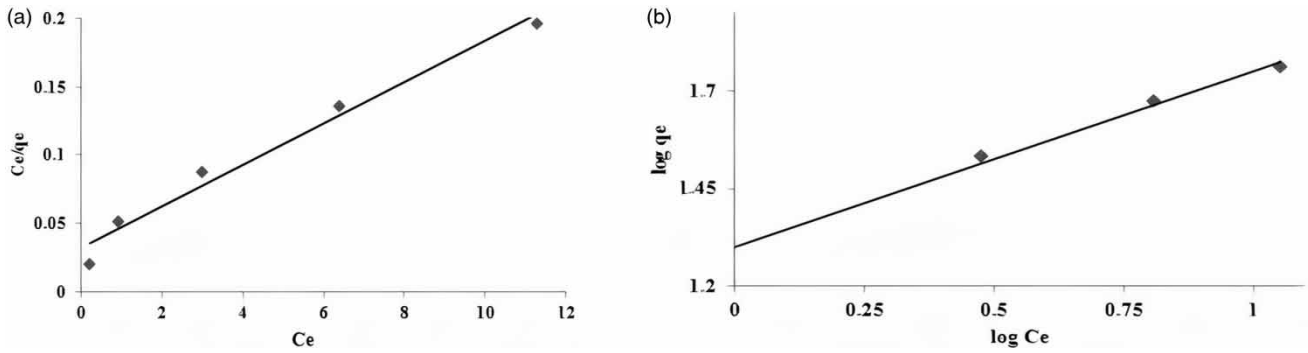

Figure 5 | Langmuir (a) and Freundlich (b) isotherm models for the adsorption of MNZ on MAC.

Table 3 | Langmuir and Freundlich isotherm model constants and correlation coefficients

Absorbent MAC	Langmuir				Freundlich		
	q_{max}	K_L	R_L	R^2	K_F	n	R^2
	66.22	0.47	0.0147	0.976	3.66	2.22	0.996

the other hand, in the Freundlich model, the value of n was greater than 1, which indicates that the adsorption of MNZ on the adsorbent was a favorable physical process. The results were consistent with the results obtained by other studies (Liu *et al.* 2012; Kong *et al.* 2016). Table 4 shows the adsorption capacity of different types of adsorbents for MNZ. The maximum absorption capacity of MAC was 66.22 mg/g. The results of the maximum adsorption capacity obtained indicated that the MAC had better performance than the other adsorbents applied.

3.6. Kinetic studies

The adsorption kinetics indicate the MNZ adsorption rate in the MAC; this adsorption rate controls the equilibrium time. To evaluate the transfer rate of MNZ mass on the adsorbent MAC, adsorption kinetics were used based on the equilibrium test data from the pseudo-first-order and pseudo-second-order models. The linear form of the pseudo-first-order kinetic model is presented by the following equation (Borna *et al.* 2016):

$$\log\ (q_e - q_t) = \log q_e - \left(\frac{k_1 t}{2.303}\right) \tag{6}$$

where q_t is the adsorption capacities at time t, and k_1 is the constant coefficient of the pseudo-first-order kinetic model.

The pseudo-second-order kinetic model is based on solid-phase adsorption. q_e and k_2 are obtained by drawing a plot of t/q_e versus t. The linear form of the model is expressed by the following equation (Rashtbari *et al.* 2020a, 2020b):

$$\frac{t}{q_e} = \frac{1}{(k_2 q_e^2)} + \left(\frac{1}{q_e}\right)t \tag{7}$$

where k_2 is the constant coefficient of the pseudo-second-order kinetic model.

Regarding the kinetic constants and the correlation coefficients (R^2) presented in Table 5 and Figure 6, as well as the comparison of experimental data with the calculated data, it can be stated that the kinetics of the adsorption followed the pseudo-second-order model. Al-Khalisy *et al.* (2010) showed that the adsorption of cephalexin from aqueous solutions by bentonite and activated carbon followed the pseudo-second-order kinetic model (Al-Khalisy *et al.* 2010).

3.7. Real wastewater samples

Real wastewater containing antibiotics contains many impurities that may interfere with the adsorption process. In this study, a real wastewater sample was obtained from the Daana Pharmaceutical Company. MNZ removal efficiency under the optimal conditions from the real wastewater sample was 64%, a lower value compared with that from the synthetic solutions.

Table 4 | Comparison of maximum adsorption capacity (q_{max}) of various adsorbents for MNZ

Adsorbent	Concentration (mg/L)	Adsorbent dose (g/L)	q_{max} (mg g^{-1})	References
Kaolin	20	1	41.34	Aleanizy *et al.* (2015)
LECA	40	1	56.31	Kalhori *et al.* (2017)
Fe-modified sepiolite	10	0.2	5.62	Ding & Bian (2015)
MgO/LECA nanocomposite	40	1	84.55	Kalhori *et al.* (2017)
Siris seed pods	–	0.5	53.194	Ahmed & Theydan (2013)
MAC	5	0.5	66.22	This study

Table 5 | Kinetics parameters of MNZ adsorption under optimal conditions and different concentrations

		Pseudo-first-order			Pseudo-second-order		
C_O (mg/L)	$q_{e,\ exp}$ (mg/g)	$q_{1,cal}$ (mg/g)	k_1 (1/min)	R_1^2	$q_{2,cal}$ (mg/g)	k_2 (g/mg·min)	R_2^2
5	10.5	6.87	0.035	0.9259	10.16	0.022	0.9909
10	18.75	15.75	0.052	0.9755	19.45	0.008	0.9852
20	36.25	30.64	0.040	0.9685	37.03	0.003	0.09712

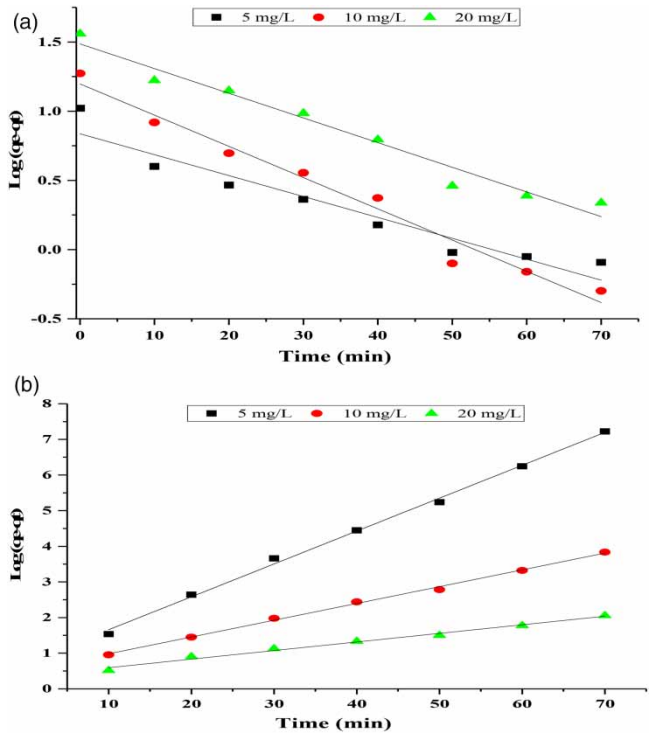

Figure 6 | Pseudo-first-order (a) and pseudo-second-order (b) for the adsorption of MNZ on MAC.

Removal efficiency in the real sample of the industrial wastewater was lower than that determined from the synthetic samples. Interfering factors such as organic and cyclic compounds as well as turbidity inside the wastewater caused the removal efficiency to decline compared with the synthetic samples. Generally, these results are suggestive of the appropriate performance of the composite in MNZ removal from the real samples (Farzadkia *et al.* 2015; Zhang *et al.* 2016).

3.8. Reusability of the adsorbent

The regeneration and recycling abilities of adsorbents are crucial for their practical application. Spent adsorbents have no benefit and are disposed of as wastes. Disposing of spent adsorbents can be difficult because some of them could be hazardous and need to be incinerated and may be toxic, flammable or even explosive (Gupta *et al.* 2013). In chemical regeneration, generally, MNZ molecules are dissolved in the eluent or get replaced by an ion-exchange process on the adsorbent surface (Pouretedal & Sadegh 2014; Chieng *et al.* 2015). The adsorption ability of MAC for the elimination of MNZ from an aqueous solution was examined by using 0.1 M NaOH as a model. As shown in Figure 7, the generation process was carried out five times. Generally, the MAC capacity for the removal of MNZ was reduced with an increasing number of regeneration cycles. Figure 7 shows that, in the first stage of regeneration, the regeneration of the adsorbent decreased to approximately 95%; however, the removal percentage after the fifth regeneration was 73%. Thus, the experimental data indicated that MAC has a high potential to be used for the adsorption of MNZ after five consecutive cycles of regeneration; it will therefore be cost-effective.

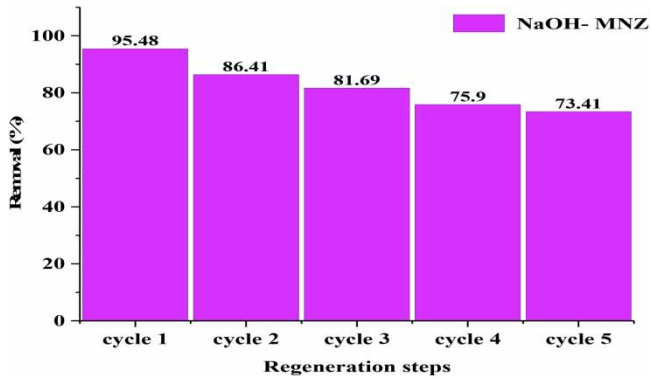

Figure 7 | Regeneration of MAC in five cycles.

4. CONCLUSIONS

In the present study, MNZ adsorption on the MAC was investigated. The results illustrated that the adsorption of MNZ had high efficiency in acidic conditions and removal performance decreased with increasing initial concentration. The study of adsorption kinetics and isotherm showed that the removal of MNZ was well proportionated with the pseudo-second-order and Freundlich models. Therefore, it can be pointed out that both physisorption and chemisorption occurred in MNZ adsorption. The surface areas of PAC and MAC were 738.18 and 706.92 m^2/g, and the total pore volumes were 0.551 and 0.532 cm^3/g. Also, the regeneration of the MAC indicated that this adsorbent has a promising capacity in five regeneration cycles for the removal of MNZ. Thus, it is concluded that MAC has a significant performance in the removal of MNZ from aquatic solutions, and it can be used for further studies of pollutant removal from water and wastewater in the laboratory and industrial scales.

ACKNOWLEDGEMENT

The authors would like to acknowledge the Baqiyatallah University of Medical Sciences for technical supports (No. IR.BMSU.REC.1398.338).

AUTHOR CONTRIBUTIONS

The authors were involved in the original idea, search and literature review, experiments, initial writing or revising the article, and with the final approval of the present article, they accept responsibility for the accuracy of its contents.

CONFLICT OF INTEREST

No potential conflict of interest was reported by the author(s).

DATA AVAILABILITY STATEMENT

All relevant data are included in the paper or its Supplementary Information.

REFERENCES

Abdollahzadeh, H., Fazlzadeh, M., Afshin, S., Arfaeinia, H., Feizizadeh, A., Poureshgh, Y. & Rashtbari, Y. 2020 Efficiency of activated carbon prepared from scrap tires magnetized by Fe_3O_4 nanoparticles: characterisation and its application for removal of reactive blue19 from aquatic solutions. *International Journal of Environmental Analytical Chemistry* 1–15. https://doi.org/10.1080/03067319.2020.1745199.

Afshin, S., Ahmad Mokhtari, S., Vosoughi, M., Sadeghi, H. & Rashtbari, Y. 2018 Data of adsorption of Basic Blue 41 dye from aqueous solutions by activated carbon prepared from filamentous algae. *Data in Brief* **21**, 1008–1013.

Afshin, S., Haghighi, M., Rashtbari, Y. & Mokhtari, S. A. 2019 Optimization of Acid Blue 113 adsorption from aqueous solutions by natural bentonite using response surface model: isotherm and kinetic study. *Journal of Health* **10** (3), 287–301.

Ahmed, M. J. & Theydan, S. K. 2012 Adsorption of cephalexin onto activated carbons from *Albizia lebbeck* seed pods by microwave-induced KOH and K_2CO_3 activations. *Chemical Engineering Journal* **211**, 200–207.

Ahmed, M. J. & Theydan, S. K. 2013 Microwave assisted preparation of microporous activated carbon from Siris seed pods for adsorption of metronidazole antibiotic. *Chemical Engineering Journal* **214**, 310–318.

Ai, L. & Jiang, J. 2010 Fast removal of organic dyes from aqueous solutions by AC/ferrospinel composite. *Desalination* **262** (1–3), 134–140.

Akbari, H. & Adibzadeh, A. 2020 Persulphate activation under UV radiation for cyclophosphamide degradation and mineralisation in aqueous solution. *International Journal of Environmental Analytical Chemistry* 1–14. https://doi.org/10.1080/03067319.2020.1817423.

Albadarin, A. B., Mangwandi, C., Ala'a, H., Walker, G. M., Allen, S. J. & Ahmad, M. N. 2012 Kinetic and thermodynamics of chromium ions adsorption onto low-cost dolomite adsorbent. *Chemical Engineering Journal* **179**, 193–202.

Aleanizy, F. S., Alqahtani, F., Al Gohary, O., Tahir, E. E. & Al Shalabi, R. 2015 Determination and characterization of metronidazole–kaolin interaction. *Saudi Pharmaceutical Journal* **23** (2), 167–176.

Alinejad, A., Akbari, H., Ghaderpoori, M., Khani Jeihooni, A. & Adibzadeh, A. 2019 Catalytic ozonation process using a MgO nano-catalyst to degrade methotrexate from aqueous solutions and cytotoxicity studies in human lung epithelial cells (A549) after treatment. *RSC Advances* **9**, 8204–8214.

Al-Khalisy, R. S., Al-Haidary, A. M. A. & Al-Dujaili, A. H. 2010 Aqueous phase adsorption of cephalexin onto bentonite and activated carbon. *Separation Science and Technology* **45** (9), 1286–1294.

Azarpira, H. & Balarak, D. 2016 Rice husk as a biosorbent for antibiotic metronidazole removal: isotherm studies and model validation. *International Journal of ChemTech Research* **9** (7), 566–573.

Bahrami Asl, F., Kermani, M., Farzadkia, M., Esrafili, A., Arian, S. S. & Zeynalzadeh, D. 2015 Removal of metronidazole from aqueous solution using ozonation process. *Journal of Mazandaran University of Medical Sciences* **24** (121), 131–140.

Baocheng, Q., Jiti, Z., Xuemin, X., Chunli, Z., Hongxia, Z. & Xiaobai, Z. 2008 Adsorption behavior of Azo Dye CI Acid Red 14 in aqueous solution on surface soils. *Journal of Environmental Sciences* **20** (6), 704–709.

Borna, M. O., Pirsaheb, M., Niri, M. V., Mashizie, R. K., Kakavandi, B., Zare, M. R. & Asadi, A. 2016 Batch and column studies for the adsorption of chromium (VI) on low-cost Hibiscus Cannabinus kenaf, a green adsorbent. *Journal of the Taiwan Institute of Chemical Engineers* **68**, 80–89.

Carrales-Alvarado, D. H., Ocampo-Pérez, R., Leyva-Ramos, R. & Rivera-Utrilla, J. 2014 Removal of the antibiotic metronidazole by adsorption on various carbon materials from aqueous phase. *Journal of Colloid and Interface Science* **436**, 276–285.

Chieng, H. I., Lim, L. B. & Priyantha, N. 2015 Sorption characteristics of peat from Brunei Darussalam for the removal of rhodamine B dye from aqueous solution: adsorption isotherms, thermodynamics, kinetics and regeneration studies. *Desalination and Water Treatment* **55** (3), 664–677.

Dantas, R. F., Rossiter, O., Teixeira, A. K. R., Simões, A. S. & Lins da Silva, V. 2010 Direct UV photolysis of propranolol and metronidazole in aqueous solution. *Chemical Engineering Journal* **158** (2), 143–147.

Ding, H. & Bian, G. 2015 Adsorption of metronidazole in aqueous solution by Fe-modified sepiolite. *Desalination and Water Treatment* **55** (6), 1620–1628.

Dong, H., Yuan, X., Wang, W. & Qiang, Z. 2016 Occurrence and removal of antibiotics in ecological and conventional wastewater treatment processes: a field study. *Journal of Environmental Management* **178**, 11–19.

Fang, Z., Chen, J., Qiu, X., Qiu, X., Cheng, W. & Zhu, L. 2011 Effective removal of antibiotic metronidazole from water by nanoscale zero-valent iron particles. *Desalination* **268** (1–3), 60–67.

Farzadkia, M., Bazrafshan, E., Esrafili, A., Yang, J.-K. & Shirzad-Siboni, M. 2015 Photocatalytic degradation of Metronidazole with illuminated TiO_2 nanoparticles. *Journal of Environmental Health Science and Engineering* **13** (1), 35.

Fazlzadeh, M., Ahmadfazeli, A., Entezari, A., Shaegi, A. & Khosravi, R. 2016 Removal of cephalexin using green montmorillonite loaded with TiO_2 nanoparticles in the presence potassium permanganate from aqueous solution. *کومش (Koomesh)* **18** (3), 388–396.

Fazlzadeh, M., Khosravi, R. & Zarei, A. 2017 Green synthesis of zinc oxide nanoparticles using *Peganum harmala* seed extract, and loaded on *Peganum harmala* seed powdered activated carbon as new adsorbent for removal of Cr(VI) from aqueous solution. *Ecological Engineering* **103**, 180–190.

Flores-Cano, J. V., Sanchez-Polo, M., Messoud, J., Velo-Gala, I., Ocampo-Pérez, R. & Rivera-Utrilla, J. 2016 Overall adsorption rate of metronidazole, dimetridazole and diatrizoate on activated carbons prepared from coffee residues and almond shells. *Journal of Environmental Management* **169**, 116–125.

Ghaedi, M., Ghayedi, M., Kokhdan, S. N., Sahraei, R. & Daneshfar, A. 2013 Palladium, silver, and zinc oxide nanoparticles loaded on activated carbon as adsorbent for removal of bromophenol red from aqueous solution. *Journal of Industrial and Engineering Chemistry* **19** (4), 1209–1217.

Gholami, Z., Ghadiri, S. K., Avazpour, M., Fard, M. A., Yousefi, N., Talebi, S. S., Khazaei, M., Saghi, M. H. & Mahvi, A. H. 2018 Removal of phosphate from aqueous solutions using modified activated carbon prepared from agricultural waste (*Populous caspica*): optimization, kinetic, isotherm, and thermodynamic studies. *Desalination and Water Treatment* **133**, 177–190.

Gupta, V. K., Kumar, R., Nayak, A., Saleh, T. A. & Barakat, M. A. 2013 Adsorptive removal of dyes from aqueous solution onto carbon nanotubes: a review. *Advances in Colloid and Interface Science* **193**, 24–34.

Hoseinzadeh, E., Rahmani, A. R., Asgari, G., Samadi, M. T., Roshanaei, G. & Zare, M. R. 2013 Application of adsorption process by activated carbon derived from scrap tires for Pb^{+2} removal from aqueous solutions. *Journal of Birjand University of Medical Sciences* **20**, 45–57.

Huang, L., Zhou, S., Jin, F., Huang, J. & Bao, N. 2014 Characterization and mechanism analysis of activated carbon fiber felt-stabilized nanoscale zero-valent iron for the removal of Cr(VI) from aqueous solution. *Colloids and Surfaces A: Physicochemical and Engineering Aspects* **447**, 59–66.

Joss, A., Zabczynski, S., Göbel, A., Hoffmann, B., Löffler, D., McArdell, C. S., Ternes, T. A., Thomsen, A. & Siegrist, H. 2006 Biological degradation of pharmaceuticals in municipal wastewater treatment: proposing a classification scheme. *Water Research* **40** (8), 1686–1696.

Jung, C., Heo, J., Han, J., Her, N., Lee, S.-J., Oh, J., Ryu, J. & Yoon, Y. 2013 Hexavalent chromium removal by various adsorbents: powdered activated carbon, chitosan, and single/multi-walled carbon nanotubes. *Separation and Purification Technology* **106**, 63–71.

Kalhori, E. M., Al-Musawi, T. J., Ghahramani, E., Kazemian, H. & Zarrabi, M. 2017 Enhancement of the adsorption capacity of the light-weight expanded clay aggregate surface for the metronidazole antibiotic by coating with MgO nanoparticles: studies on the kinetic, isotherm, and effects of environmental parameters. *Chemosphere* **175**, 8–20.

Kermani, M., Asl, F. B., Farzadkia, M., Esrafili, A., Arian, S. S., Arfaeinia, H. & Dehgani, A. 2013 Degradation efficiency and kinetic study of metronidazole by catalytic ozonation process in presence of MgO nanoparticles. *The Journal of Urmia University of Medical Sciences* **24** (10), 839–850.

Khosravi, R., Zarei, A., Heidari, M., Ahmadfazeli, A., Vosughi, M. & Fazlzadeh, M. 2018 Application of ZnO and TiO_2 nanoparticles coated onto montmorillonite in the presence of H_2O_2 for efficient removal of cephalexin from aqueous solutions. *Korean Journal of Chemical Engineering* **35** (4), 1000–1008.

Kong, Q., Wang, Y.-n., Shu, L. & Miao, M.-s. 2016 Isotherm, kinetic, and thermodynamic equations for cefalexin removal from liquids using activated carbon synthesized from loofah sponge. *Desalination and Water Treatment* **57** (17), 7933–7942.

Kümmerer, K., Al-Ahmad, A. & Mersch-Sundermann, V. 2000 Biodegradability of some antibiotics, elimination of the genotoxicity and affection of wastewater bacteria in a simple test. *Chemosphere* **40** (7), 701–710.

Legnoverde, M. S., Simonetti, S. & Basaldella, E. I. 2014 Influence of pH on cephalexin adsorption onto SBA-15 mesoporous silica: theoretical and experimental study. *Applied Surface Science* **300**, 37–42.

Liu, W., Xie, H., Zhang, J. & Zhang, C. 2012 Sorption removal of cephalexin by HNO_3 and H_2O_2 oxidized activated carbons. *Science China Chemistry* **55** (9), 1959–1967.

Moussavi, G., Alahabadi, A., Yaghmaeian, K. & Eskandari, M. 2013 Preparation, characterization and adsorption potential of the NH_4Cl-induced activated carbon for the removal of amoxicillin antibiotic from water. *Chemical Engineering Journal* **217**, 119–128.

Nasseh, N., Barikbin, B., Taghavi, L. & Nasseri, M. A. 2019 Adsorption of metronidazole antibiotic using a new magnetic nanocomposite from simulated wastewater (isotherm, kinetic and thermodynamic studies). *Composites Part B: Engineering* **159**, 146–156.

Pereira, M. F. R., Soares, S. F., Órfão, J. J. & Figueiredo, J. L. 2003 Adsorption of dyes on activated carbons: influence of surface chemical groups. *Carbon* **41** (4), 811–821.

Pérez, T., Garcia-Segura, S., El-Ghenymy, A., Nava, J. L. & Brillas, E. 2015 Solar photoelectro-Fenton degradation of the antibiotic metronidazole using a flow plant with a Pt/air-diffusion cell and a CPC photoreactor. *Electrochimica Acta* **165**, 173–181.

Pittman Jr., C. U., He, G.-R., Wu, B. & Gardner, S. D. 1997 Chemical modification of carbon fiber surfaces by nitric acid oxidation followed by reaction with tetraethylenepentamine. *Carbon* **35** (3), 317–331.

Pouretedal, H. R. & Sadegh, N. 2014 Effective removal of Amoxicillin, Cephalexin, Tetracycline and Penicillin G from aqueous solutions using activated carbon nanoparticles prepared from vine wood. *Journal of Water Process Engineering* **1**, 64–73.

Rahmani, A. R., Shabanloo, A., Fazlzadeh, M., Poureshgh, Y. & Vanaeitabar, M. 2019 Optimization of sonochemical decomposition of ciprofloxacin antibiotic in US/PS/nZVI process by CCD-RSM method. *Desalination and Water Treatment* **145**, 300–308.

Rashtbari, Y., Hazrati, S., Azari, A., Afshin, S., Fazlzadeh, M. & Vosoughi, M. 2020a A novel, eco-friendly and green synthesis of PPAC-ZnO and PPAC-nZVI nanocomposite using pomegranate peel: Cephalexin adsorption experiments, mechanisms, isotherms and kinetics. *Advanced Powder Technology* **31** (4), 1612–1623.

Rashtbari, Y., Afshin, S., Hamzezadeh, A., Abazari, M., Poureshgh, Y. & Fazlzadeh, M. 2020b Application of powdered activated carbon coated with zinc oxide nanoparticles prepared using a green synthesis in removal of Reactive Blue 19 and Reactive Black-5: adsorption isotherm and kinetic models. *Desalination and Water Treatment* **179**, 354–367.

Rivera-Utrilla, J., Prados-Joya, G., Sánchez-Polo, M., Ferro-García, M. A. & Bautista-Toledo, I. 2009 Removal of nitroimidazole antibiotics from aqueous solution by adsorption/bioadsorption on activated carbon. *Journal of Hazardous Materials* **170** (1), 298–305.

Rivera-Utrilla, J., Sánchez-Polo, M., Prados-Joya, G., Ferro-García, M. A. & Bautista-Toledo, I. 2010 Removal of tinidazole from waters by using ozone and activated carbon in dynamic regime. *Journal of Hazardous Materials* **174** (1), 880–886.

Samarghandi, M. R., Al-Musawi, T. J., Mohseni-Bandpi, A. & Zarrabi, M. 2015 Adsorption of cephalexin from aqueous solution using natural zeolite and zeolite coated with manganese oxide nanoparticles. *Journal of Molecular Liquids* **211**, 431–441.

Shafeeyan, M. S., Daud, W. M. A. W., Houshmand, A. & Arami-Niya, A. 2011 Ammonia modification of activated carbon to enhance carbon dioxide adsorption: effect of pre-oxidation. *Applied Surface Science* **257** (9), 3936–3942.

Shemer, H., Kunukcu, Y. K. & Linden, K. G. 2006 Degradation of the pharmaceutical metronidazole via UV, Fenton and photo-Fenton processes. *Chemosphere* **63** (2), 269–276.

Shokoohi, R., Samadi, M. T., Amani, M. & Poureshgh, Y. 2018a Modeling and optimization of removal of cefalexin from aquatic solutions by enzymatic oxidation using experimental design. *Brazilian Journal of Chemical Engineering* **35** (3), 943–956.

Shokoohi, R., Samadi, M. T., Amani, M. & Poureshgh, Y. 2018b Optimizing laccase-mediated amoxicillin removal by the use of Box–Behnken design in an aqueous solution. *Desalination and Water Treatment* **119**, 53–63.

Stöhr, B., Boehm, H. P. & Schlögl, R. 1991 Enhancement of the catalytic activity of activated carbons in oxidation reactions by thermal treatment with ammonia or hydrogen cyanide and observation of a superoxide species as a possible intermediate. *Carbon* **29** (6), 707–720.

Su, J., Huang, H.-G., Jin, X.-Y., Lu, X.-Q. & Chen, Z.-L. 2011 Synthesis, characterization and kinetic of a surfactant-modified bentonite used to remove As(III) and As(V) from aqueous solution. *Journal of Hazardous Materials* **185** (1), 63–70.

Sun, L., Chen, D., Wan, S. & Yu, Z. 2018 Adsorption studies of dimetridazole and metronidazole onto biochar derived from sugarcane bagasse: kinetic, equilibrium, and mechanisms. *Journal of Polymers and the Environment* **26** (2), 765–777.

Wang, Y., Gao, B.-y., Yue, W.-w. & Yue, Q.-y. 2007 Preparation and utilization of wheat straw anionic sorbent for the removal of nitrate from aqueous solution. *Journal of Environmental Sciences* **19** (11), 1305–1310.

Wang, H., Zhang, G. & Gao, Y. 2010 Photocatalytic degradation of metronidazole in aqueous solution by niobate $K_6Nb_{10.8}O_{30}$. *Wuhan University Journal of Natural Sciences* **15** (4), 345–349.

Wang, X., Du, Y. & Ma, J. 2016 Novel synthesis of carbon spheres supported nanoscale zero-valent iron for removal of metronidazole. *Applied Surface Science* **390**, 50–59.

Watkinson, A. J., Murby, E. J. & Costanzo, S. D. 2007 Removal of antibiotics in conventional and advanced wastewater treatment: implications for environmental discharge and wastewater recycling. *Water Research* **41** (18), 4164–4176.

Xu, W., Zhao, Q., Wang, R., Jiang, Z., Zhang, Z., Gao, X. & Ye, Z. 2017 Optimization of organic pollutants removal from soil eluent by activated carbon derived from peanut shells using response surface methodology. *Vacuum* **141**, 307–315. https://doi.org/10.1016/j.vacuum.2017.04.031.

Zarei, A. A., Tavassoli, P. & Bazrafshan, E. 2018 Evaluation of UV/S_2O_8 process efficiency for removal of metronidazole (MNZ) from aqueous solutions. *Water Science and Technology* **2017** (1), 126–133.

Zhang, C., Lai, C., Zeng, G., Huang, D., Yang, C., Wang, Y., Zhou, Y. & Cheng, M. 2016 Efficacy of carbonaceous nanocomposites for sorbing ionizable antibiotic sulfamethazine from aqueous solution. *Water Research* **95**, 103–112.

First received 4 July 2021; accepted in revised form 5 October 2021. Available online 20 October 2021